High-resolution study of ^{208}Pb with 35-MeV protons*

W. T. Wagner, G. M. Crawley, G. R. Hammerstein, and H. McManus
Cyclotron Laboratory and Physics Department, Michigan State University, East Lansing, Michigan 48824
(Received 16 May 1974; revised manuscript received 15 January 1975)

The inelastic scattering of 35-MeV protons by ^{208}Pb was measured with a resolution of 5–8 keV. Angular distributions of states up to an excitation energy of about 8 MeV were obtained. Collective model calculations enabled the l transfers of many states to be identified. The possibility of excitation of 1^+ states is discussed. Microscopic model calculations were made with both phenomenological and theoretical information. The large number of observed unnatural parity states permitted the role of noncentral forces in these transitions to be investigated.

[NUCLEAR REACTIONS ^{208}Pb(p,p), $E=35$ MeV; measured $\sigma(\theta)$, $\theta=10$–$100°$. Deduced L, $\beta_L{}^2$. Microscopic DWBA analysis.]

I. INTRODUCTION

Nuclei in the mass region about ^{208}Pb have been extensively studied both experimentally and theoretically. Inelastic scattering[1-6] and Coulomb excitation[7] have given information about the strongly populated states of many of these nuclei Decay studies and transfer reactions[8-11] together with isobaric analog resonance experiments[12-14] have provided information about the microscopic structure of many of the low-lying states. The level properties and the microscopic configurations have been intensively studied in nuclear structure calculations. Also, recent improvements[15] in the theoretical treatment of inelastic proton scattering, primarily use of realistic interactions and explicit inclusion of knock-on exchange effects, have led to successful calculations for cases in which wave functions or transition densities were well known. ^{208}Pb thus is an attractive subject for a high resolution (p,p') experimental study coupled with a microscopic theoretical analysis.

A relatively high resolution ^{208}Pb(p,p') experiment[1] was reported at 24.5 MeV bombarding energy with energy resolution of ≈ 25 keV full width at half-maximum (FWHM). Spin and parity assignments for the most strongly excited states up to 4.7 MeV of excitation energy were made. Lately, analysis[2] of the (p,p') reaction at 54 MeV has extended l transfer assignments to states up to about 7 MeV of excitation, where ^{208}Pb becomes particle unstable. The resolution was about 35–40 keV FWHM. In both studies, experimental angular distributions were compared primarily with the collective model predictions. To date, these represent the most extensive and highest resolution (p,p') studies of ^{208}Pb. Recently, experiments with charged particle reactions at energies of 30 to 50 MeV and resolution better than 10 keV have become possible. This permits the extraction of cross sections and excitation energies for weakly excited states which can be reliably compared with theoretical predictions.

This paper reports a high resolution study of ^{208}Pb(p,p') performed at 35 MeV with energy resolution on the order of 1 part in 5000. Angular distributions at this bombarding energy have more distinguishing features than those at lower energies yet are not so forward-angle peaked as to make identification of small l transfers difficult. About 150 states with excitation energies up to 7.5 MeV have been experimentally resolved and their angular distributions are presented. Determinations of l assignments and deformation parameters as well as comparison with previous measurements are made. Microscopic model inelastic scattering predictions are compared with the data for normal and nonnormal parity excitations. The existence of magnetic dipole states is also discussed.

II. EXPERIMENTAL PROCEDURE

The experiment used the 35 MeV proton beam from the Michigan State University sector-focused cyclotron, and the scattered protons were detected using the Enge split-pole spectrometer. The high resolution data was recorded on Kodak NTB 25 μm nuclear emulsions in the spectrometer focal plane. A thin stainless steel absorber between 0.25 and 0.38 mm thick immediately before the emulsion stopped all particles other than protons. The absorber decreased the particle

energy, thus enhancing track brightness and did not significantly broaden the line width. On-line determination of the focal plane linewidth using the "speculator" technique of Blosser *et al.*[16] was used to optimize the resolution initially and to monitor it during data collection. Targets of about 100 $\mu g/cm^2$ thickness were used throughout the high resolution study and were prepared by vacuum evaporation on a 15–20 $\mu g/cm^2$ carbon foil with a substrate of one or two layers of Formvar. The plate data resolution ranged from 5 to 8 keV (FWHM) and a typical spectrum is displayed in Fig. 1.

To complement the high resolution data, states strongly excited in inelastic scattering were first studied using a single-wire proportional counter[17] in the spectrometer focal plane. A 6.0 mg/cm^2 self-supporting foil, made by rolling, served as the target. The lead used in all target fabrication was isotopically enriched to 99.14% ^{208}Pb and was obtained from the Oak Ridge National Laboratory. Resolution of about 45 keV allowed cross sections for the first 3^-, 2^+, 4^+, 6^+, and 8^+ levels as well as the first two 5^- states to be measured. Both plate and counter data were measured relative to elastic events monitored with a NaI(Tl) detector at a scattering angle of 90° which lies near a relative maximum in the elastic cross section for ^{208}Pb. The normalization from the NaI detector agreed to within 10% with the normalization using the integrated beam current.

Absolute normalization of the counter data was done by comparison of the optical model using Becchetti-Greenlees[18] best-fit parameters with the measured elastic angular distribution. Comparing the plate data with the counter results thus determined the normalization of the plate data. Absolute normalization of the counter and plate data is believed good to about 5 and 10%, respectively. Whenever possible, the more extensive counter results are displayed although both sets of data were measured in the range of 10 to 100°.

III. DATA

A. Excitation energies

Clearly resolved states of ^{208}Pb, ^{16}O, and ^{12}C with well-known excitation energies were used in the energy calibration.[19] A few iterations were performed until the input calibration energies agreed with the average predicted energies. The results of all observed states are tabulated in Table I and the energies used for the calibration are indicated. For comparison the excitation en-

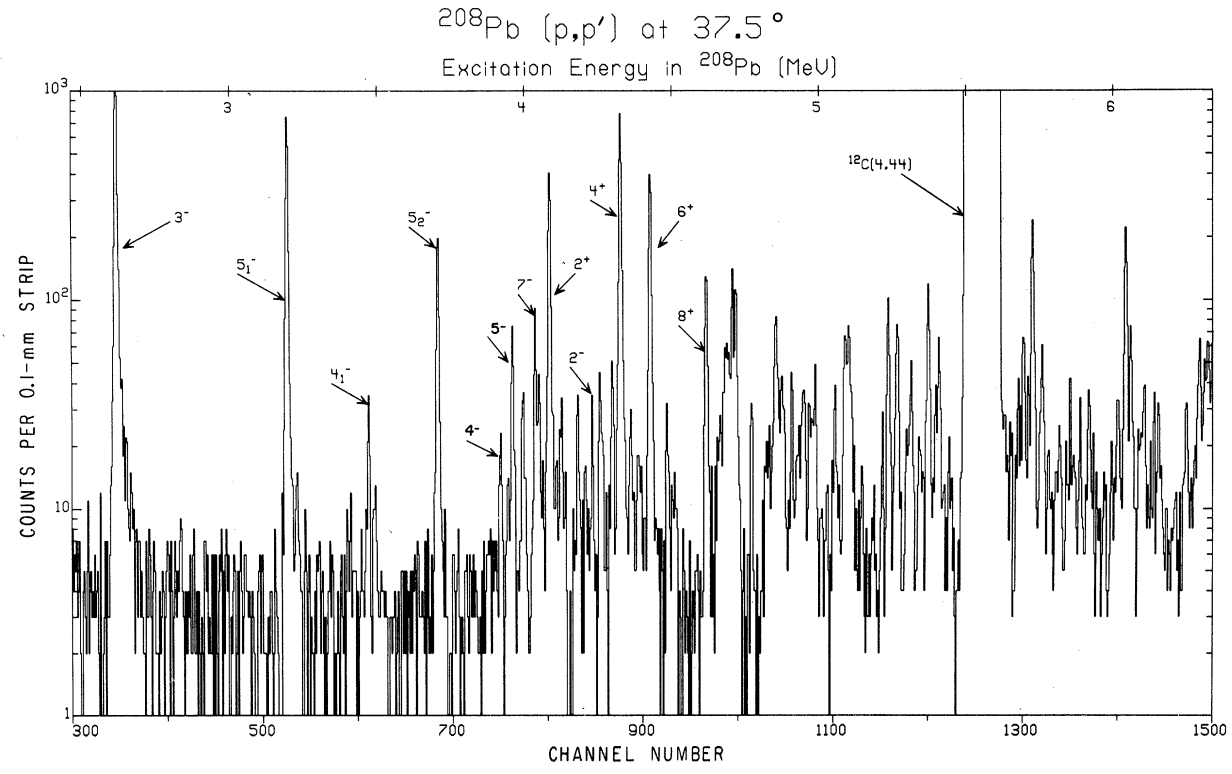

FIG. 1. Typical spectrum of protons scattered by ^{208}Pb. The resolution is about 6 keV.

TABLE I. Energy levels, l transfers, and deformation parameters for ^{208}Pb.

Present work			54 MeV(p,p') (Ref. 2)			Compilation (Ref. 20)		Shell model study (Ref. 21)	
$E_x \pm \Delta E_x$ (MeV)	L	β_L	E_x (MeV)	L	β_L [a]	E_x (MeV)	J^π	E_x (MeV)	J^π
2.6146 [b]	3	0.120	2.615	3	0.108	2.6146	3^-		
3.1978 [b]	5	0.058	3.198	5	0.055	3.1977	5^-	3.198	5^-
3.475 ± 0.001	$J^\pi = 4^-$ [c]		3.475			3.4750	4^-	3.475	4^-
3.7087 [b]	5	0.034	3.709	5	0.035	3.7085	5^-	3.709	5^-
						3.73?			
						3.76?			
3.919 ± 0.001	$J^\pi = 4^-$ [c]		3.922?			3.9202	$(6)^-$	3.919	4^-
3.946 ± 0.003						3.946			
3.961 ± 0.001	(5)	0.018	3.959			3.9609	$(4)^-$	3.960	5^-
3.995 ± 0.004	$J^\pi = 6^-$ [c]					3.9985		3.996	6^-
4.037 ± 0.001	(7)	0.038	4.028	≥6		4.038	$(7)^-$	4.035	7^-
4.054 ± 0.003	(3)	0.013				4.050	(4)	4.049	3^-
4.0855 [b]	2	0.058	4.086	2	0.058	4.086	2^+		
4.106 ± 0.003	(3)	0.010							
4.125 ± 0.001	$J^\pi = 4^-$ [c]					4.1254	$4^-, 5^-$	4.126	4^-
4.141 ± 0.003	(2)	0.0084							
4.159 ± 0.004	(2)	0.0067	4.150			4.155?			
4.181 ± 0.001	(5)	0.018				4.1805	$(5)^-$	4.180	5^-
4.206 ± 0.002	$J^\pi = 6^-$ [c]					4.204	$5^-, 6^-$	4.205	6^-
4.230 ± 0.002	$J^\pi = 2^-$ [c]		4.240	5	0.017	4.231	(2^-)	4.230	2^-
						4.253	$(2^-, 4^-)$	4.255	3^-
4.256 ± 0.002 [d]						4.258	$(4^-, 5^-)$	4.256	4^-
								4.261	5^-
4.296 ± 0.002	5	0.018				4.2961	$(5)^-$	4.296	5^-
4.3237 [b]	4	0.067	4.324	4	0.069	4.323	4^+		
4.357 ± 0.003	$J^\pi = 4^-$ [c]					4.357	(4^-)	4.360	4^-
4.385 ± 0.003	$J^\pi = 6^-$ [c]					4.382	$(6)^-$	4.388	6^-
4.403 ± 0.002	(3)	0.0084							
	(4)	0.0077							
4.4235 [b]	6	0.062	4.420	6	0.064	4.425	(6^+)		
4.444 ± 0.004	(5)	0.0089							
4.463 ± 0.004	(2)	0.0056							
4.480 ± 0.001 [d]	$J^\pi = 6^-$ [c]		4.50			4.4804	$(6)^-$	4.482	6^-
4.577 ± 0.005									
4.610 ± 0.001	8	0.040	4.606	(8)	0.039	4.608	$(8)^+$		
4.680 ± 0.002	(9)	0.016							
4.698 ± 0.001	3	0.033	4.696	3	0.037	4.6982	$(3)^-$	4.700	3^-
4.711 ± 0.002						4.709			
4.762 ± 0.002	7	0.015	4.749						
4.841 ± 0.002	$J^\pi = 1^-$ [e]		4.847	(1)	≤0.008	4.840	(1)		
						4.859	0^+		
4.863 ± 0.002 [d]						4.863	$(7)^+$		
4.895 ± 0.002	≈10	≈0.027	4.897	10	0.022	4.91	$(4-10)^+$		
4.917 ± 0.003	≥6								
4.933 ± 0.003	4	0.024	4.937	(4)	0.026	4.934	(2^+)		
4.954 ± 0.004	3	0.017				4.953?	(4–6)		
4.973 ± 0.003	3	0.026				4.973	$(3)^-$		
4.991 ± 0.004	≥8		4.983	(6)	0.022				
5.010 ± 0.003	9	0.017							
5.036 ± 0.003	$J^\pi = 2^-$ [c]					5.038	$(2)^-$		
5.072 ± 0.003	(9)	0.039	5.079	10	0.030	5.077	$(5-10)^+$		
5.087 ± 0.004	3	0.033							
5.128 ± 0.003			5.110			5.127	$(2, 3)^-$		
5.163 ± 0.004						5.16			
5.194 ± 0.004	3 [f]	0.016 [f]				5.20	$(8-10)^+$		
5.214 ± 0.003			5.205	4	0.032,	5.211			
				3	0.028				

TABLE I *(Continued)*

Present work			54 MeV(p, p') (Ref. 2)			Compilation (Ref. 20)		Shell model study (Ref. 21)	
$E_x \pm \Delta E_x$ (MeV)	L	β_L	E_x (MeV)	L	β_L [a]	E_x (MeV)	J^π	E_x (MeV)	J^π
						5.236	0^+		
5.242 ± 0.003			5.235	(3)	0.035	5.2446	$(2,3)^-$		
5.274 ± 0.005	3	0.013				5.281	0^-		
5.291 ± 0.003	$J^\pi = 1^-$ [e]					5.289	1^-		
5.321 ± 0.004	3	0.017							
5.345 ± 0.003	3	0.035	5.342	3	0.039	5.344			
5.370 ± 0.006	5	0.016							
5.383 ± 0.003						5.381			
5.417 ± 0.004 [d]	(6)	0.015,				5.41			
	(7)	0.016							
5.444 ± 0.005	≥6								
5.483 ± 0.003	5	0.045				5.482			
						5.507	1^-		
5.514 ± 0.005 [d]	1 and 3	0.038(3)	5.515	(3)	0.055				
5.542 ± 0.004	3	0.032				5.542			
						5.550	(2^+)		
5.564 ± 0.003	2	0.017				5.563	(1, 2)		
5.596 ± 0.006						5.599	(3^-)		
5.615 ± 0.004	≥6								
						5.629	(2^+)		
5.642 ± 0.004 [d]									
5.658 ± 0.003	5	0.022				5.652			
5.673 ± 0.004	(3)	0.016							
5.689 ± 0.003	4	0.045	5.690	4	0.051	5.685			
5.720 ± 0.004 [d]	7	0.027				5.709			
5.743 ± 0.004	9	0.019							
5.763 ± 0.005	6	0.013							
5.777 ± 0.004 [d]						5.777	(3)		
5.796 ± 0.005						5.801	(2^+)		
5.813 ± 0.004	3	0.028	5.808	(3)	0.026	5.810			
5.842 ± 0.006 [d]						5.833			
5.872 ± 0.005 [d]	(3)	0.015				5.874	$(3)^-$		
5.898 ± 0.004	(8)	0.016							
5.923 ± 0.005	$J^\pi = 2^-$ [c]					5.922	$(2)^-$		
5.948 ± 0.006						5.942	1^-		
5.966 ± 0.004	≈9	≈0.027				5.967	$(4)^-$		
5.993 ± 0.003	6	0.049	5.988	3	0.044,				
				4	0.0048				
6.010 ± 0.004	3	0.027				6.006	$(3, 4^-)$		
6.035 ± 0.005									
6.052 ± 0.004	4	0.015				6.058			
6.082 ± 0.005						6.083	$(2)^-$		
6.099 ± 0.004									
6.170 ± 0.007	2	0.0071				6.172	(2^+)		
6.191 ± 0.005	3	0.020							
6.214 ± 0.004									
6.233 ± 0.005 [d]									
6.248 ± 0.005 [d]	(7)	0.029	6.245	7	0.037	6.244			
6.261 ± 0.006 [d]	$J^\pi = 1^-$ [e]					6.258	(1)		
6.276 ± 0.004									
6.314 ± 0.005	(3)	0.015				6.311	1^-		
6.332 ± 0.006	6	0.025							
6.353 ± 0.006 [d]									
6.381 ± 0.006 [d]	≈7	≈0.020							
6.393 ± 0.006									
6.423 ± 0.006 [d]									
6.443 ± 0.006 [d]	7	0.024							

TABLE I *(Continued)*

Present work			54 MeV(p,p') (Ref. 2)			Compilation (Ref. 20)		Shell model study (Ref. 21)	
$E_x \pm \Delta E_x$ (MeV)	L	β_L	E_x (MeV)	L	β_L [a]	E_x (MeV)	J^π	E_x (MeV)	J^π
6.458 ± 0.005									
6.483 ± 0.006 [d]									
6.529 ± 0.006 [d]	(5)	0.026							
6.544 ± 0.006									
6.572 ± 0.005									
6.588 ± 0.005									
6.615 ± 0.005	3	0.023							
	4	0.026							
6.631 ± 0.005									
6.658 ± 0.005	4	0.023	6.525	≈7	≈0.033				
6.688 ± 0.005	5	0.041	6.675	≥6					
6.720 ± 0.006 [d]									
6.737 ± 0.005 [d]									
6.786 ± 0.006									
6.801 ± 0.005									
6.823 ± 0.007									
6.843 ± 0.006	(8)	0.021							
6.862 ± 0.006									
6.876 ± 0.005 [d]									
6.925 ± 0.006 [d]	4	0.020							
6.940 ± 0.006									
6.965 ± 0.008	$J^\pi = 1^-$ [e]								
6.992 ± 0.006	(3)	0.019							
7.019 ± 0.007	(3)	0.021							
7.046 ± 0.006									
7.061 ± 0.005									
7.080 ± 0.006									
7.114 ± 0.007	(3)	0.020							
7.174 ± 0.005 [d]									
7.192 ± 0.006	(4)	0.022							
7.219 ± 0.008									
7.239 ± 0.005	$J^\pi = 1^-$ [e]								
7.268 ± 0.008									
7.302 ± 0.008 [d]	5	0.018							
7.325 ± 0.117 [d]									
7.343 ± 0.006									
7.382 ± 0.009	(4)	0.016							
7.404 ± 0.008 [d]									
7.549 ± 0.008									
7.573 ± 0.007									
7.594 ± 0.007 [d]									
7.684 ± 0.009									
7.723 ± 0.008									
8.166 ± 0.008									

[a] Obtained from the transition rates G_L using $\beta_L = [4\pi(2L+1)G_L/Z^2(3+L)^2]^{1/2}$.
[b] Level used in energy calibration.
[c] Spin and parity adopted from previous work of Refs. 20 or 21.
[d] Level with probable multiplet structure.
[e] Identified by similarity of angular distributions. Previous work (Refs. 10, 14, and 20) gives these as 1^- levels.
[f] Multiplet: β_L and L given for apparently dominant member.

ergies determined by previous work are also given. The energies listed are from the results of a Nuclear Data compilation,[20] the recent 54 MeV (p,p') experiment,[2] and an intensive study by Heusler and von Brentano[21] of states below about 4.5 MeV. As may be seen, the final values for the calibration reference levels are in excellent agreement with prior measurements involving

$(d,p\gamma)$ and $(n,n'\gamma)$ high resolution work. The general agreement with previous determinations is good and appears to extend up to about 7 MeV of excitation.

Due to kinematic broadening and to the displacements of the focal planes of protons scattered from different mass nuclei, the oxygen and carbon contaminant peaks appear wide in the lead spectra and these centroids are somewhat poorly determined.

The highest-lying ^{208}Pb state used in the calibration was the 4.423 MeV level. Thus the energies above 4.5 MeV are obtained by extrapolation. The errors in Table I reflect this. For states lying below 4.5 MeV the standard deviation in the measured energy is given as the error. Above 4.5 MeV, however, the given error includes an addition of 1.0 keV for each MeV of excitation to the statistical error to account for extrapolation as well as the uncertainties due to the increasing level density and the smaller cross sections.

Most states below 5 MeV of excitation appear to be completely resolved. The 3.73 and 3.76 MeV levels reported in early ^{207}Pb(d,p) experiments[8] were not seen here and an upper limit of about 40 μb/sr can be set for excitation of these states by proton scattering at this energy. These states have not been observed in subsequent studies with either transfer or inelastic scattering reactions.

The angular distribution for the 4.256 MeV

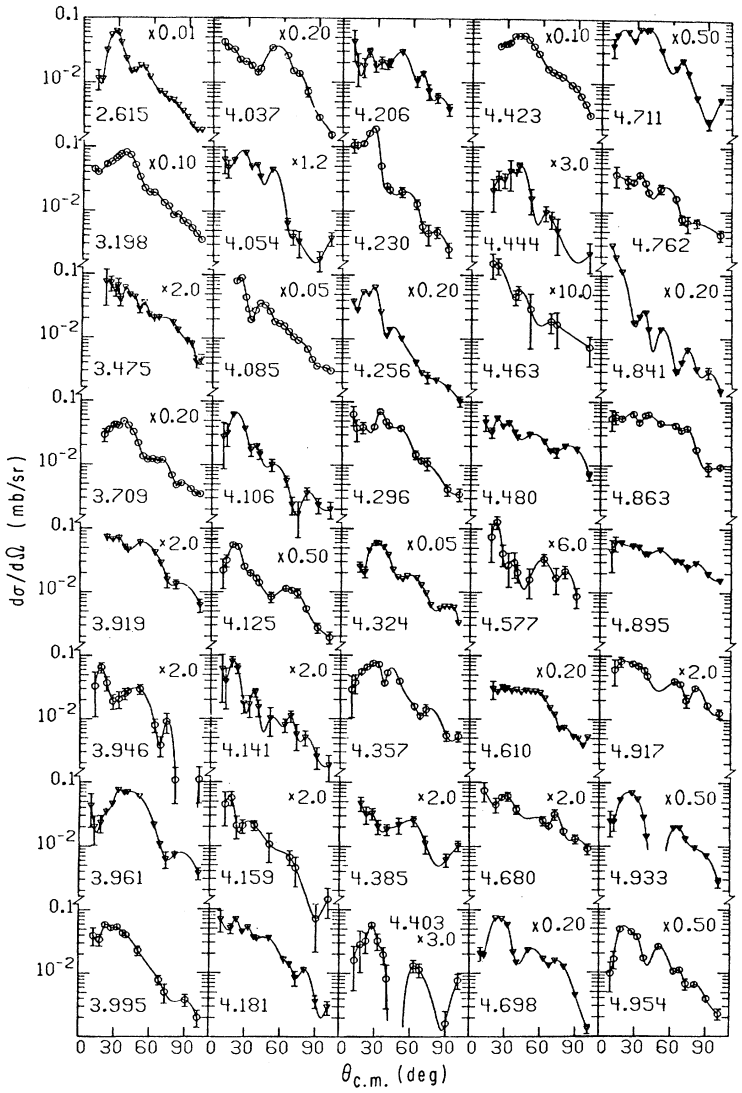

FIG. 2. Measured inelastic cross sections. The lines drawn through the data points are merely to guide the eye and do *not* represent fits to the data. The energies of the levels are given in MeV.

multiplet, seen in Fig. 2, is fairly well structured but cannot be fitted with a single l transfer, suggesting an unresolved multiplet. A 4.251 MeV level has been seen in a (p,t) and (t,p) study at 20 MeV with 17 KeV resolution performed by Igo, Barnes, and Flynn.[9] A state at 4.253 MeV has been observed in $(d,p\gamma)$ studies.[10] Neither work indicated the possibility of multiplet structure. A possible doublet at about this excitation has been seen in isobaric resonance work[12] with 9–13 keV resolution. If the energy corrections of Ref. 20 are applied to the data of Ref. 12, the members of this doublet lie at 4.253 and 4.259 MeV. Of course, different reactions can be expected to populate different nuclear levels. Heusler and von Brentano[21] using shell model systematics and a global compilation of experimental results, have concluded that this region of excitation energy contains a 4.255, 4.256, and 4.261 MeV triplet with $J^\pi = 3^-$, 4^-, and 5^-, respectively.

Most of the states above 5 MeV appear to be completely resolved, but those states whose widths indicate possible multiplet structure have been indicated in Table I. In general, the poor statistics and narrow line shape prohibit reliable fitting with numerical techniques. The level at 5.194 MeV was revealed as a doublet at several angles. The previously reported 5.236–5.245 MeV doublet was not resolved. The level seen here at 5.242 MeV has no apparent doublet structure,

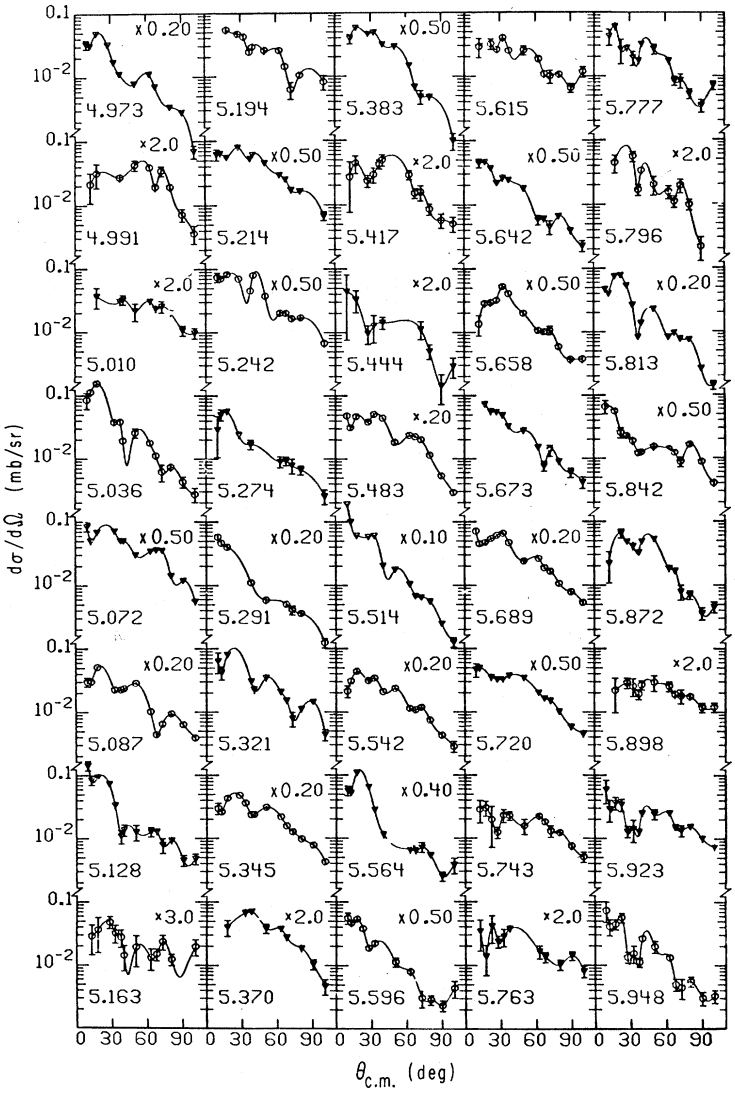

FIG. 3. Measured inelastic cross sections. The lines drawn through the data points are merely to guide the eye and do *not* represent fits to the data. The energies of the levels are given in MeV.

suggesting that the 5.236 MeV level is not populated here.

Interestingly, eight states were not found that had been previously reported: the 4.859, 4.968, 5.550, 5.629, 5.801, 5.862, 5.937, and 5.973 MeV levels. These states were seen in two-neutron transfer by Igo *et al.*[9] and have been identified as configurations with predominant 2p-2h admixtures. That these states are not excited in (p,p') is consistent with viewing inelastic proton scattering as mediated by a one-body operator.

B. Inelastic angular distributions

The angular distributions for all resolved peaks resulting from inelastic scattering are shown in Figs. 2 through 5. The cross sections are displayed with their corresponding excitation energies. The error bars indicate statistical errors and were drawn only when greater than the symbol size. It should be emphasized that the curves passing through the data in these figures have been drawn merely as a guide and do *not* represent theoretical fits to the curves. Gaps in the angular distributions at certain angles are due to obstruction of the peaks of interest by reaction products from the various contaminants in the target.

Since the plate results were normalized by comparison to the counter data, normalization errors due to unresolved states in the counter data should

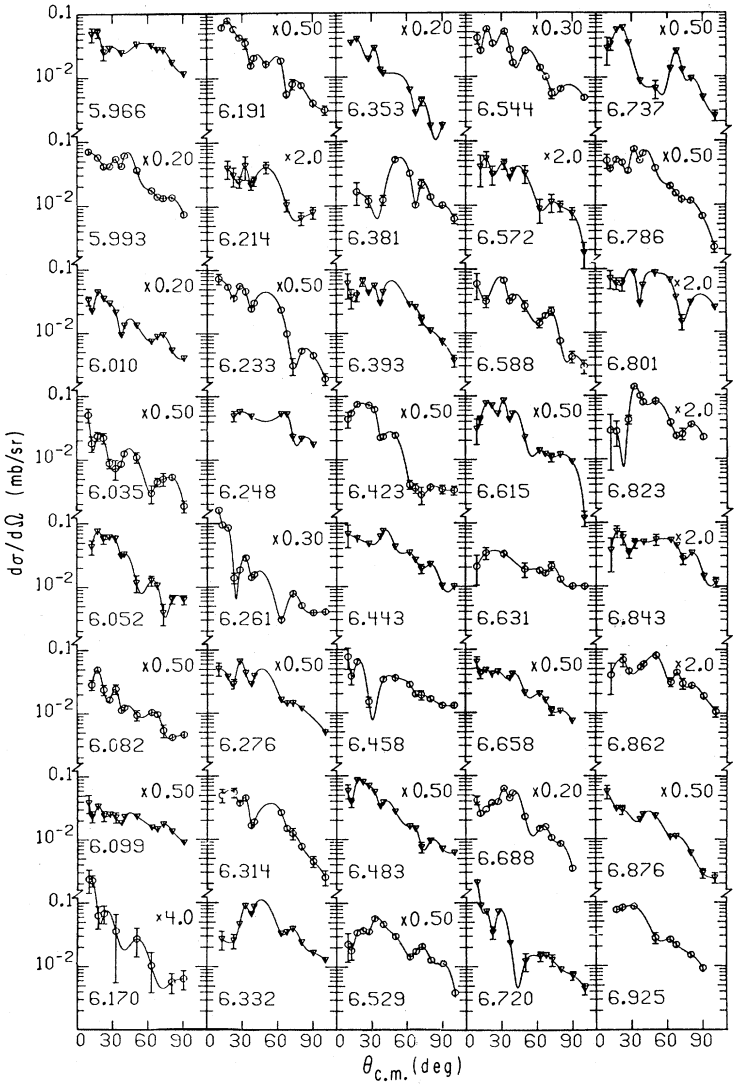

FIG. 4. Measured inelastic cross sections. The lines drawn through the data points are merely to guide the eye and do *not* represent fits to the data. The energies of the levels are given in MeV.

be considered. The first 3^- and first and second 5^- levels, that is, the levels emphasized in the normalization, were completely resolved in both sets of data. In the counter data the 2^+, 4^+, 6^+, and 8^+ states were sometimes only partially separated from nearby levels, but had cross sections about 20 times larger than those of the neighboring levels. Thus the final plate-to-counter normalization can contain no more than 5% error from this source.

C. Discussion of the collective model

The distorted-wave Born-approximation (DWBA) collective model (CM) uses a deformed optical potential as the form factor for inelastic scattering. The optical potentials are usually obtained from fits to elastic scattering data, and a number of sets of parameters for ^{208}Pb in this energy region have been determined.[6,22-25] Figure 6 displays the 35 MeV proton elastic scattering angular distribution as measured with the wire counter. Also shown are results of elastic scattering calculations done using Becchetti-Greenlees (BG) best-fit optical parameters and parameters obtained from a search on the data with the code GIBELUMP.[26] The search was initialized with BG values and performed with the spin-orbit parameters fixed at the BG values. The two calculations are in good agreement with the data and differ only slightly from each other.

For the extraction of deformation parameters presented in this paper BG parameters were chosen both for entrance and exit channel optical potentials and for form factors, since they are given as a function of energy and so allow the use of exit channel parameters appropriate to a given outgoing particle energy.

Some additional calculations were performed for l transfers of 2, 4, and 6 using two different sets of parameters. In both cases BG parameters were employed for the exit channel optical poten-

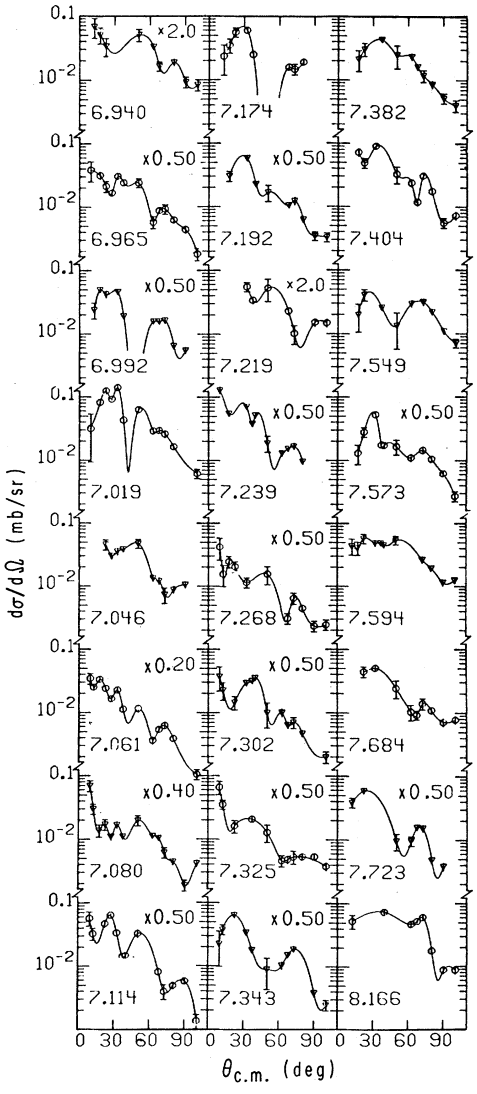

FIG. 5. Measured inelastic cross sections. The lines drawn through the data points are merely to guide the eye and do *not* represent fits to the data. The energies of the levels are given in MeV.

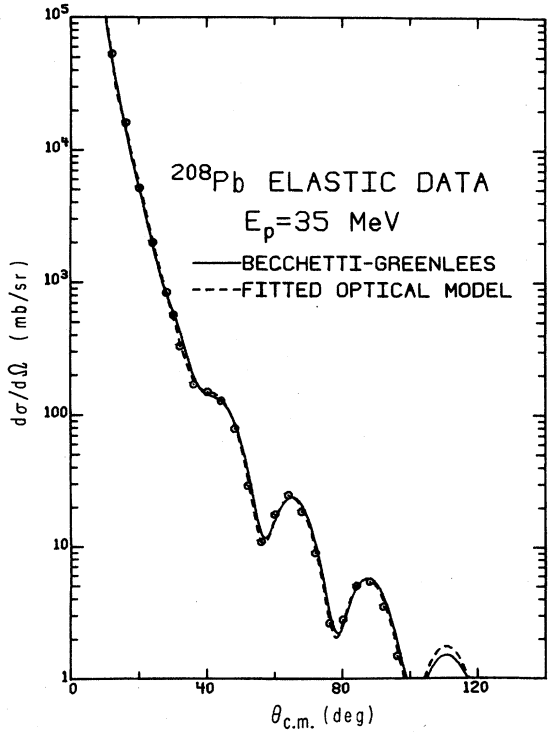

FIG. 6. Comparison of the measured elastic angular distribution with calculations described in the text.

tial. In one case BG parameters, and in the other case fitted parameters, were used for the form factor and entrance channel optical potential. At each l value the cross section calculated with the fitted parameters was 30% larger than that calculated with the BG parameters, primarily because of the effect on the form factor of a much deeper surface imaginary well depth in the fitted set. This calculation is not quite consistent due to the mismatch in entrance and exit channel optical parameters, but it does indicate a sensitivity to the optical parameters which should be borne in mind in assessing the precision of the deformation parameters.

D. l transfers and deformation parameters

Collective model calculations were performed with the code DWUCK[27] using the BG optical parameters. Tests involving Q-value dependence of the cross sections indicated little sensitivity and a $Q = -5$ MeV was assumed for each l transfer for each calculation. Coulomb excitation was included in the $L = 2$ and 3 cases, although only the smaller l transfer receives notable contribution from this mode of excitation. The fits to the states are displayed in Figs. 7 and 8. The L assignments were made by comparing the experimental angular distributions both with theoretical angular distributions and with angular distributions of states of well determined spin and parity. The β_L's were obtained from $\beta_L{}^2 = \sigma_{\text{exp}}/\sigma_{\text{th}}$. Both the β_L and l-transfer assignments are given in Table I for comparison with the measurements of Ref. 2. Where possible those states with angular distributions of unidentifiable shape have J^π adopted from the work of Ref. 20 or Ref. 21.

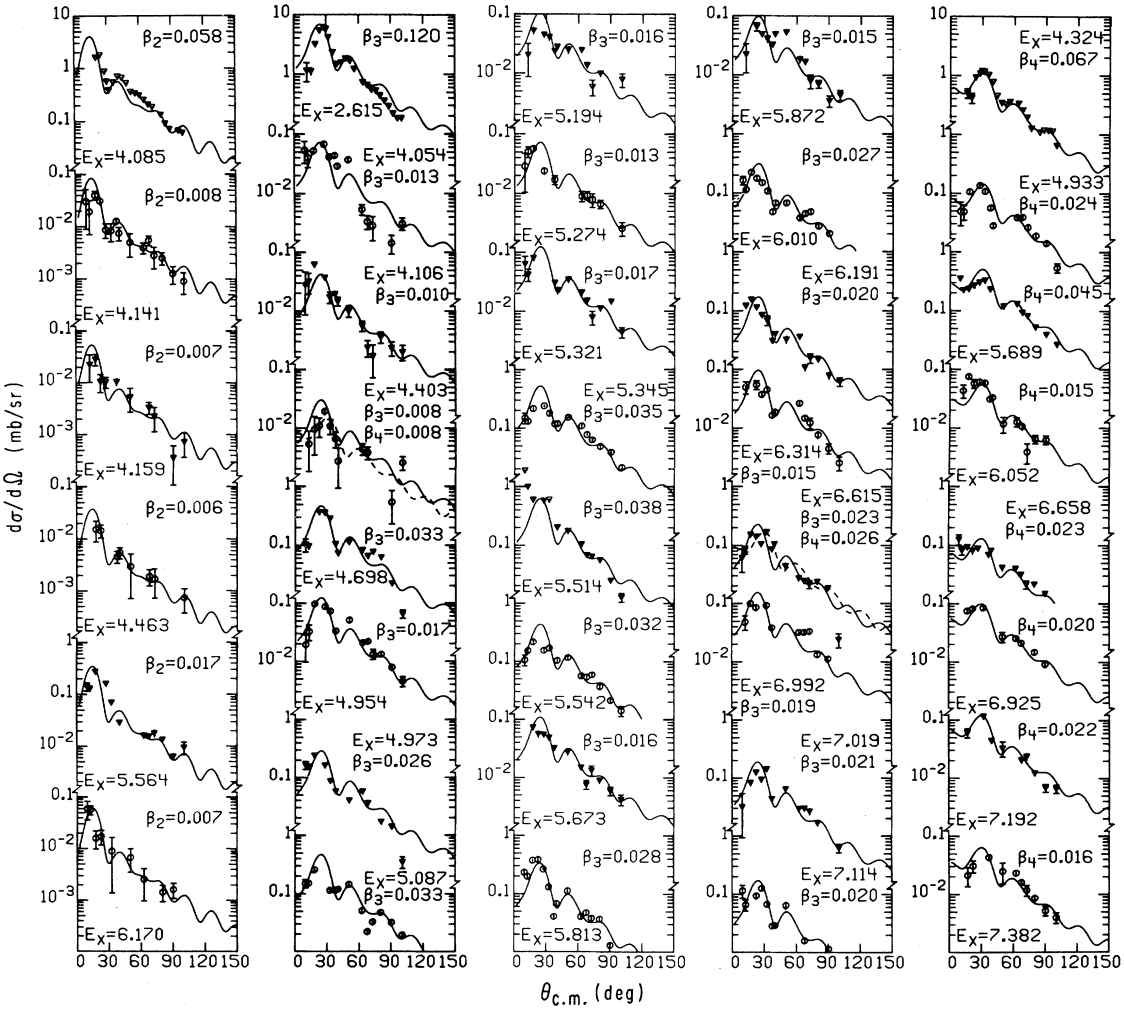

FIG. 7. Collective model fits for all identified states. Displayed with the fits are the excitation energy of the state and the deformation parameter β_L corresponding to orbital angular momentum transfer L.

Deformation prameters for states in ^{208}Pb which have been measured by (p,p') at a number of energies are compared in Table II. They appear to decrease with increasing proton energy. However, a careful analysis of a large body of scattering data would be necessary in order to draw any significant conclusion concerning energy dependence of the the β_L's.

1. 1^- states

The levels at 4.841, 5.291, 6.261, 6.965, and 7.239 MeV have fairly similar angular distributions, as seen in Fig. 9. All are fairly strongly forward peaked and have angular distributions that oscillate together in phase. These levels have been identified[10,20] as electric dipole levels and the data appears consistent with these assignments.

States near 5.94 and 6.31 MeV, seen in $(d,p\gamma)$ measurements, were reported to be 1^-. A two-neutron transfer experiment[9] also tentatively reported 1^- levels at 7.176, 7.319, 7.387, 7.480, and 7.523 MeV of excitation energy. Our data display no marked similarity in angular distribution of levels near these excitations with those of the levels definitely identified as 1^-.

A 5.505 MeV state seen in a resonant $(p,p'\gamma)$ study[14] was assigned a spin of 1^- on the basis of its ground state γ decay strength. ^{207}Pb$(d,p\gamma)$ results[10] indicated a 1^- level at 5.506 MeV, as did the two-neutron transfer study of Ref. 9. However, the 54 MeV inelastic proton study[2] found an unresolved doublet at 5.515 MeV and assigned a tentative 3^- spin. We observe an apparent multiplet at 5.514 MeV which has a large forward angle cross section, like the 4.841 and 6.261 MeV states,

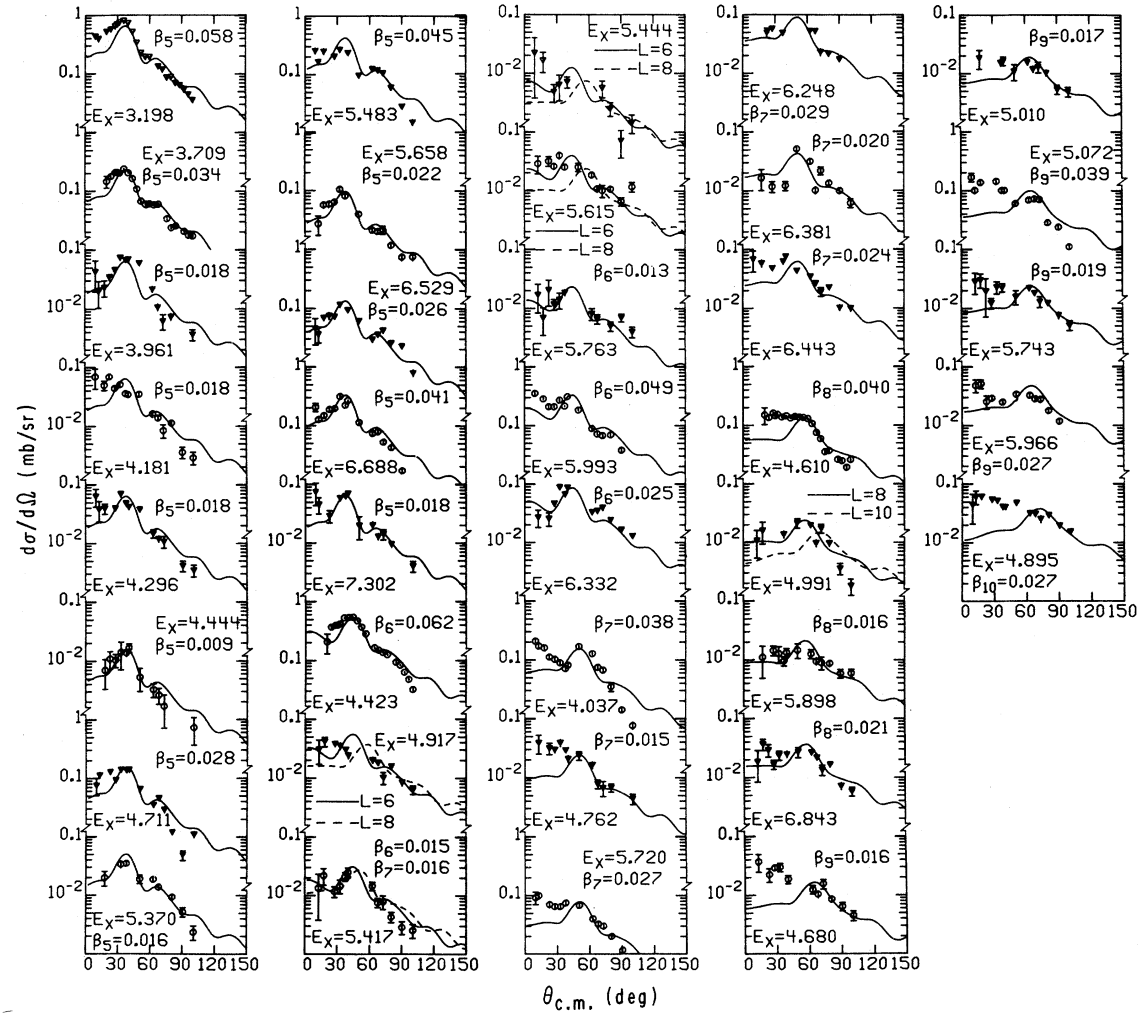

FIG. 8. Collective model fits for all identified states. Displayed with the fits are the excitation energy of the state and the deformation parameter β_L corresponding to orbital angular momentum transfer L.

TABLE II. Summary of deformation parameters from (p,p') studies.

E_p (MeV) \ E_x (MeV), J	2.615 3^-	3.198 5^-	3.709 5^-	4.085 2^+	4.324 4^+	4.423 6^+	4.610 8^+
24.5 [a]	0.12	0.072	0.034	0.058	0.066	0.057	0.045
30 [b]	0.13						
30.3 [c]	0.11						
31.0 [d]	0.13						
35.0 [e]	0.126	0.058	0.034	0.058	0.067	0.062	0.040
40 [f]	0.11						
40 [g]	0.11	0.059		0.059			
54 [h]	0.11	0.055	0.035	0.058	0.069	0.064	0.039
61 [i]	0.098	0.043	0.027	0.053	0.062	0.055	0.039

[a] Reference 1.
[b] Reference 24.
[c] Reference 6.
[d] Reference 22.
[e] Present work.
[f] Reference 23.
[g] Reference 4.
[h] Reference 2.
[i] Reference 5.

but is fitted well at larger angles by an $L=3$ characteristic shape. These facts suggest that this excitation is a doublet with dipole and octupole members.

2. *Search for 1^+ states*

Recently some attention has been given to the search for magnetic dipole states in heavy nuclei.[28,29] A 180° (e,e') experimental study[29] reported states at 6.2 and 7.9 MeV which were identified as 1^+ with transition widths of 11 and 44 eV, respectively. Theoretical studies[30-32] predict wave functions for the first two 1^+ states in ^{208}Pb which are dominated by two spin-flip components, $n(i_{11/2},i_{13/2}^{-1})$ and $p(h_{9/2},h_{11/2}^{-1})$. The wave functions of Broglia, Molinari, and Sorenson,[30] which were used in the present calculations, attribute nearly equal amplitudes to these components, with like signs ($\Delta T \simeq 0$) for the lower state and opposite signs ($\Delta T \simeq 1$) for the higher. The predicted transition widths are 2 and 80 eV, as compared with the experimental values of 11 and 44 eV, but a 10–15% mixing of the wave functions yields values in agreement with experiment because of the large difference in the nucleon isoscalar and isovector magnetic moments, which enter the transverse magnetic (e,e') form factors.

Our data reveal states at 6.23 and 8.01 MeV whose forward angle peaking and nearness to the states seen in (e,e') mark them as likely candidates for 1^+ assignments. The 8.01 MeV level is obscured by contaminants and other Pb levels at most angles, but a full angular distribution was obtained for the 6.23 MeV state. This angular distribution is compared in Fig. 10 with a calculation which employed techniques described in Sec. IV C, which used the Broglia wavefunction and the nucleon-nucleon forces described in Sec. IV B. Four theoretical curves are shown. The two dashed curves correspond to using central forces

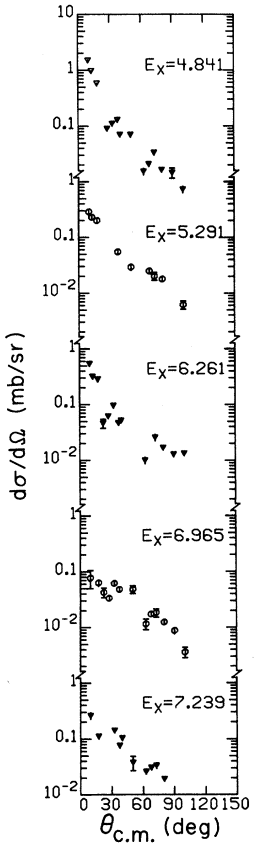

FIG. 9. Data for those states which have been previously identified as 1^- levels.

only, with and without exchange (from wave function antisymmetrization). The two solid curves include the effect of noncentral forces (tensor and two-nucleon spin-orbit). Calculations including exchange, which are more realistic, are distinguished by asterisks suitably placed. Both magnitude and shape of the experimental cross section are well reproduced by the calculation that included exchange and noncentral forces. It is seen that the effect of exchange is important, that central forces are dominant, but that there is an appreciable exchange contribution from the noncentral forces. A very similar cross-section magnitude and angular distribution are predicted for the higher lying level, assuming the Broglia wave function is nearly correct, as excitation by protons of this spin-flip transition is dominated almost completely by the proton component of the excited state, which is roughly the same for both levels. For the same reason mixing of the Broglia wave functions, which merely alters the relative phase of the neutron and proton components, has little effect on proton excitation but drastic effects on electromagnetic excitation.

We conclude that identification of the 6.23 MeV state as 1^+ is sound, and that further experimental study may well confirm a 1^+ identification for the 8.01 MeV level also.

3. 2^+ states

We have identified six probable quadrupole levels. The well-known 2^+ state at 4.085 MeV is a dominant feature of any inelastic proton spectrum. Two nearby states at 4.141 and 4.159 MeV are also tentatively identified as $L=2$ states and it seems fairly certain that the excitations at 4.463, 5.564, and 6.170 MeV are also 2^+ states. The observed 2^+ states have about 20% of the total expected strength given by an energy-weighted sum rule (ESR).[33]

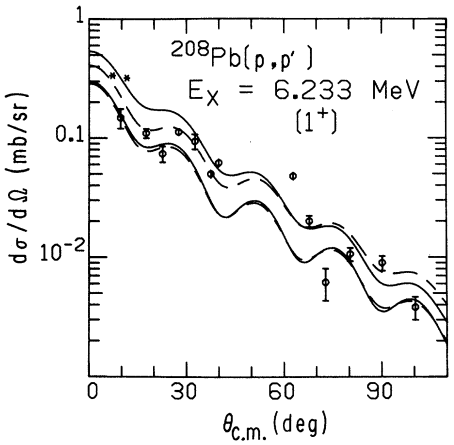

FIG. 10. Angular distribution for the 6.233 MeV level. The solid lines correspond to calculations done with both central and noncentral forces; the dashed curve show results with only a central force. The asterisks indicate calculations including exchange effects. The curves without the asterisks show the direct contribution to the cross section only.

4. 3^- levels

Many transitions involving angular momentum transfers of 3 were observed and transition strengths were extracted for them. The first excited state, with transition strength of 39.6 single particle units (s.p.u.), exhausts about 20% of an ESR,[33] revealing it as a truly collective state. Totally, the observed 3^- excitations contribute about 50% to the isoscalar octupole ESR strength predicted for ^{208}Pb. Further, the observed 3^- strength is quite fractionated and many of the levels identified were previously unreported.

5. 4^+ levels

The collective model fits to the well-known 4.324 MeV level and other $L=4$ levels are shown in Fig. 7. The angular distribution of the 4.403 and 6.615 MeV states are fitted equally well by $L=3$ or $L=4$ characteristic shapes so that the l transfer is not uniquely determined for these levels. The level at 5.689 MeV is quite collective with a transition strength of about 6 s.p.u.

6. 5^- states

The first two 5^- levels at 3.198 and 3.709 MeV are very collective with deformation parameters corresponding to transition rates of 10.5 and 3.6 s.p.u., respectively; the states at 5.483 and 6.688 MeV have inelastic transition rates of 6.3 and 5.2 s.p.u., respectively, revealing a rather large concentration of strength at high excitation. The 3.961 MeV level was previously suggested to be a 4^- unnatural parity excitation with possible doublet properties.[20] Our assignment of 5^- is in agreement with the conclusions of Refs. 9 and 21.

7. 6^+ states

Besides the well-known 6^+ 4.424 MeV level, other levels with shapes corresponding to $L=6$ were found. There is some ambiguity in assigning a spin of 6 to the 5.417 MeV level, as it is probably equally well described by an $L=7$ shape. The 4.917, 5.444, and 5.615 MeV levels apparently involve l transfers of 6, but an exact assignment cannot be made.

8. States with $L \geq 7$

Transitions with large l transfer have angular distributions which fall off less rapidly and whose maxima occur at larger angles than those involving small l transfer. For $L \leq 6$ these two features generally make an assignment failry unambiguous but for $L \geq 7$ the distinction is not so clear. The data for the 4.037 MeV level, for example, has a maximum near 60° fitted by $L=7$ or $L=8$ curves but has a very rapid falloff so that a J^π of 7^- is preferred for this level. Reference 12 has suggested a (7^-, 6^-) doublet at this energy, while Ref. 9 identified a 7^- state, both supporting our identification. As exemplified by this state (Fig. 8, also Figs. 14 and 17) and as noted by Lewis, Bertrand, and Fulmer,[2] the predicted collective model cross section for large angular momentum transfer usually underestimates the forward angle data, the difference between the data and the theory apparently being greater for the high spin cases. This fact and the lack of distinct shapes for states with spins larger than 6 makes l-transfer identification tentative.

IV. APPLICATIONS OF THE MICROSCOPIC MODEL

A. Comparison with (e,e') for strongly excited states

Inelastic electron scattering allows the proton portion of the transition density to be determined fairly unambiguously. Unfortunately, (e, e') gives little information about the neutron motion in nuclear excitations. However, for strongly collective normal parity excitations it is plausible[34,35] to assume that the transition density for neutrons is related to that for protons by

$$\rho_n = (N/Z)\rho_p \ .$$

Bernstein[34] has shown this prescription to work well for inelastic α scattering.

In applying this prescription to (p,p') we have assumed that the spin-flip and noncentral forces contribute negligibly in transitions to the normal parity states. The DWBA form factor F^{J0J} for transition to a state of spin J was obtained following Ref. 35. Basically,

$$F^{J0J}(r) = \int_0^\infty \left[V_{pp}^{J0J}(r, r') + \frac{N}{Z} V_{pn}^{J0J}(r, r') \right] \rho_p(r') r'^2 dr' \ ,$$

where ρ_p is the proton transition density obtained from (e, e'). V_{pp}^{J0J} and V_{pn}^{J0J} are the strengths of the Jth multipole of the proton-proton and proton-neutron interactions, respectively. Here, the projectile-target interaction was taken to be an effective bound state interaction (G matrix) obtained from the long range part of the Hamada-Johnston potential cut off at the separation distance of 1.05 fm. The zero-range approximation of Petrovich[36] was adopted to account for knock-on exchange effects.

The first 2^+, 4^+, 6^+, and 3^- as well as the first two 5^- levels were examined. Charge transition densities, with the exception of that of the 6^+ level, were obtained from the work of Nagao and Torizuka[37] and of Heisenberg and Sick.[38] Since the effect of the finite proton size is small in heavy nuclei, this correction was neglected and for each transition the proton density was taken to be the experimental charge density. For the 6^+ level, since the experimental best fit parameters were not reported,[37] the (e, e') data for this level was fitted using a transferred-momentum-corrected Born approximation. The density had the radial form

$$\rho_p^J(r) = N r^{J-1} \frac{d}{dr} \left[1 + \exp\left(\frac{r - C}{A} \right)^2 \right]^{-1} \ ,$$

where N is related to the $B(EJ)$ for the transition, and C and A are the usual nuclear surface param-

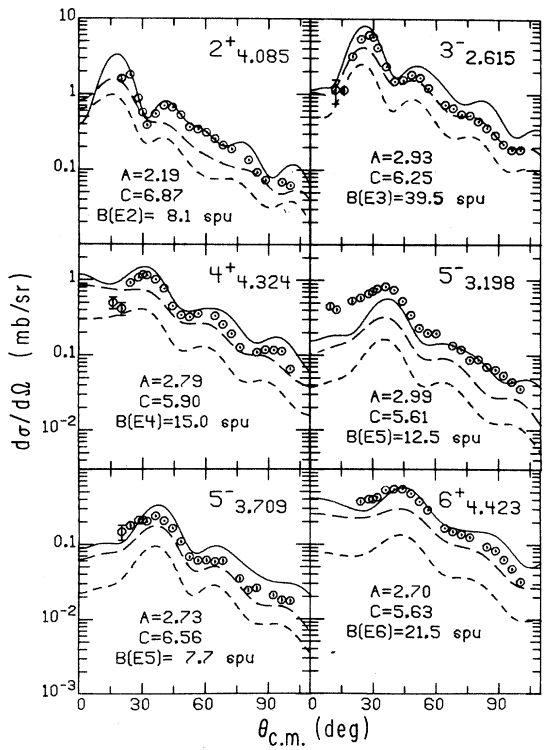

FIG. 11. Results of calculations for the strongly excited states seen in both (p, p') and (e, e'). The lower and upper dashed curves correspond to calculations with and without the exchange approximation, respectively. The solid curve includes complex coupling effects as explained in the text.

TABLE III. RPA and phenomenological wave functions for the lowest 2^-, 4^-, and 6^- states of ^{208}Pb.

	Neutron configurations							Proton configurations			
	$2g_9$-$2f_5^{-1}$	$2g_9$-$3p_1^{-1}$	$2g_9$-$3p_3^{-1}$	$2g_9$-$2f_7^{-1}$	$3d_5$-$3p_1^{-1}$	$3d_5$-$2f_5^{-1}$	$3d_5$-$3p_3^{-1}$	i_{11}-$3p_1^{-1}$	$1h_9$-$3d_3^{-1}$	$1h_9$-$3s_1^{-1}$	$2f_7$-$2d_3^{-1}$
2^- (RPA)	0.954	...	...	0.117	−0.179	−0.073	...	...	...	...	0.130
2^- (Phenom.)	−0.029	...	...	0.013	−0.010	−0.001	...	...	...	...	−0.005
	−0.980	...	...	...	−0.210	0.025	0.045	...	...	...	...
4^- (RPA)	−0.071	0.988	0.121	...	...	...	...	...	...	...	...
	−0.009	−0.012	0.007	...	...	...	...	...	...	...	...
4^- (Phenom.)	−0.158	−0.921	−0.245	−0.060	...	...	...	...	0.119	−0.023	...
6^- (RPA)	0.995	...	0.074	...	...	...	...	...	...	...	...
	−0.006	...	−0.006	...	...	...	...	...	...	...	...
6^- (Phenom.)	−0.871	...	0.101	0.030	...	...	...	0.329	0.346	...	...

eters.

For the 3^- level the transition density of Heisenberg and Sick gives a $B(E3)$ in good agreement with the $\beta_3 = 39.6$ s.p.u. extracted here using the CM (Sec. III D 4) and with that obtained in a recent analysis of all available (e, e') data[37-40] on this state. The parameters of the transition density for each state considered are given in Fig. 11.

The results of these calculations are given in Fig. 11. The dashed curves show results with (long dash) and without (short dash) the exchange contributions.

The theoretical curves including exchange (long dash) correspond qualitatively to experiment, but fall systematically below the experimental data. In other studies of (pp')[41] improved fits have been obtained by adding an imaginary component to the form factor obtained from the collective model . The solid curves show the results obtained by adding such an imaginary part to the real form factor. The imaginary part was taken to be the CM form factor obtained from the imaginary part of the BG optical potential, with a deformation parameter such that when applied to the real CM form factor from the real part of the BG optical potential it reproduced the cross section (long dash) previously calculated from the G-matrix force and $(e - e')$ data. Since the 2^+ state is the only one of these states significantly excited by the Coulomb interaction, the solid curve for this state includes both complex coupling and Coulomb excitation. By including this imaginary component in the form factor, agreement with experiment is improved; if anything, the cross sections are slightly overestimated. The first 5^- state is the only level underestimated by these calculations. If the (e, e') data of Friedrich[40] are used for this state, the theoretical cross section is increased but the (p, p') data is still underestimated. This indicates that the neutron and proton transition densities are not in the assumed ratio of $N:Z$. Indeed, the wave function used in the calculations in Sec. IV C has a neutron density larger than N/Z times the proton transition density and gives a better prediction of this state's inelastic strength.

For the other levels the slight overestimation is consistent with the use of the zero-range exchange approximation.[36] Further, the prescription used for the complex coupling is highly phenomenological in that it assumes a direct relation between the imaginary part of the inelastic form factor and the imaginary part of the empirical optical potential. It probably represents an upper limit on the imaginary part of the form factor.

In conclusion, these results generally support the assumptions about the ratio of the neutron and proton densities and the dominance of the central

non-spin-flip forces in collective excitations. The transition to the first 5^- state suggests that these assumptions may not always be true.

B. Phenomenological wave functions

Heusler and von Brentano,[21] using a global compilation of ^{208}Pb data involving particle transfer, γ-ray, and (p,p') resonant data, have examined the excitation-energy region in ^{208}Pb up to about 4.7 MeV, and have deduced from the empirical evidence the particle-hole structure of many of the states, including the amplitudes, and, with some uncertainty, the phases of the various components. Microscopic model calculations were carried out using these empirical wave functions. The wave-function components for the lowest 2^-, 4^-, and 6^- states are given in Table III. The code DWBA70[42] which treats knockon exchange exactly was used. The central part of the effective interaction used was Serber mixture with strengths of $-30:10:10:10$ (MeV), and the radial form was was taken to be a 1 fm range Yukawa. This effective force has been found[43-45] to be a good representation of the phenomenological force determined by fitting definitive reaction data and reproduces the effects of the long range part of the Hamada-Johnston interaction used in Sec. IV A. The tensor force was taken from the work of Crawley *et al.*[46] and of Fox and Austin.[47] This study assumed that the tensor isoscalar portion was zero. The $L\cdot S$ force was taken from studies by Fox and Austin.[47] In all cases considered, the spin-orbit force contributed negligibly to the cross sections.

The harmonic oscillator wave functions used had an oscillator parameter b set to 2.47 fm, a value consistent with ^{208}Pb(e,e_0) results. Again, BG parameters were used for the entrance and exit channel optical parameters. As for the 1^+ level (Fig. 10), four curves are shown for each state. The two dashed curves correspond to using central forces only, with and without exchange (from wave function antisymmetrization). The two solid curves include the effect of noncentral forces (tensor and two-nucleon spin orbit). Calculations including exchange, which are more realistic, are distinguished by asterisks suitably placed.

The states considered include normal parity excitations, the 3^- states at 4.054 and 4.698 MeV, 5^- at 3.198, 3.709, 3.961, and 4.181 MeV, and 7^- at 4.037 MeV, and nonnormal parity excitations, the 2^- state at 4.230 MeV, 4^- at 3.475, 3.919, and 4.125 MeV, and 6^- at 3.995, 4.206, and 4.385 MeV. The normal parity states are mostly moderately collective. The calculation underestimates their strength consistently by mainly large factors ~5, indicating that the strength in these states comes from a large number of configurations, each with

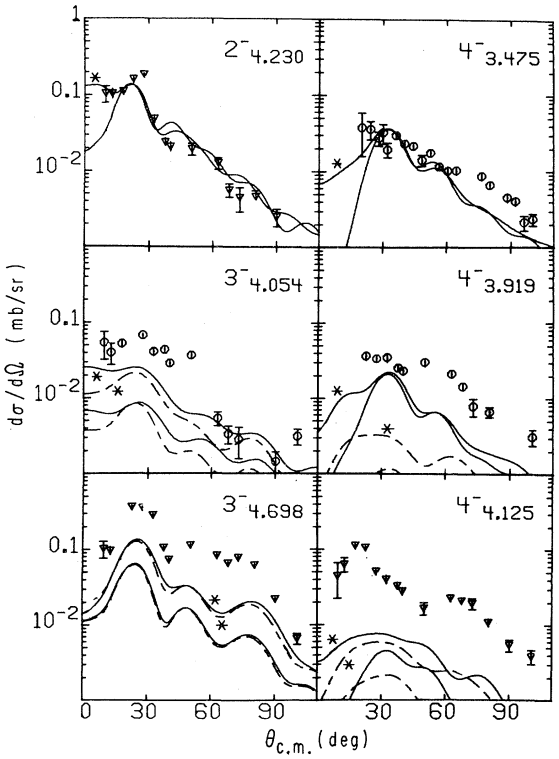

FIG. 12. The calculations using phenomenological wave functions for the states shown. The meaning of the asterisks is the same as in Fig. 10.

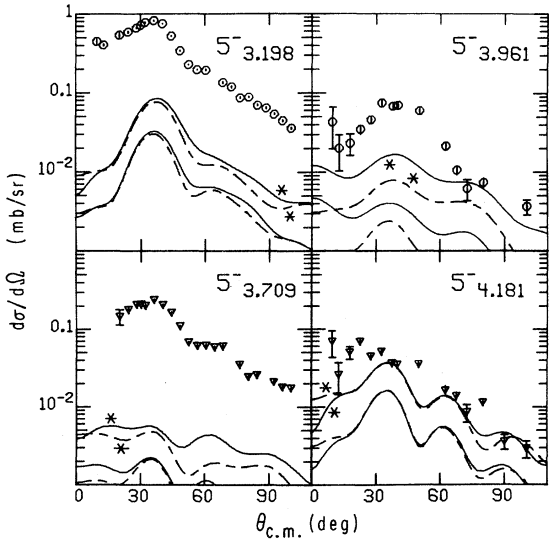

FIG. 13. The calculations using phenomenological wave functions for the states shown. The meaning of the asterisks is the same as in Fig. 10.

small amplitude, that are not detected by spectroscopic analysis. Also, for these states noncentral forces play an insignificant role and exchange is very important. Results are shown for the 3^- states in Fig. 12, for the 5^- states in Fig. 13, and for the 7^- state in Fig. 14.

On the other hand, for nonnormal parity states the tensor force is much more important, giving the entire cross section for the lowest 2^- and 4^- states.

Theoretically, the first 2^- and 6^- states are predominately from the $2g_{9/2}$-$2f_{5/2}^{-1}$ neutron configuration. The prediction for the 2^- (Fig. 12) fits the data moderately well. The 6^- (Fig. 14) agrees neither in magnitude nor shape. In both cases the tensor force is dominant.

The cross sections of the first three 4^- states are also shown in Fig. 12. The first 4^- level has a dominant $(2g_{9/2}$-$3p_{1/2}^{-1})$ neutron configuration and has been observed in analog experiments[12,13,48] and in (d,p) experiments.[8-11] It corresponds to the lowest shell model state arising from breaking the $3p_{1/2}$ neutron pair. The prediction for this state is in good agreement with the data: for the second and third states the calculation underestimates the data. The theoretical distributions for the first two 4^- levels are characteristic of an l transfer of 5 due to the large contribution of the tensor force which favors the higher of the allowed l transfers.

C. Theoretical wave functions

The purity[49] of double shell closure in ^{208}Pb makes shell model calculations[32,50,51] practicable and many such are available for the description of the states. Here we use the random phase approximation (RPA) vectors of Gillet, Green, and Sanderson[32] and of Kuo.[51] The states considered fall into three groups. The first consists of even natural parity excitations of which the first two 2^+ states and the first 4^+ and 6^+ states are considered. For these the wave functions of Gillet *et al.*[32] were used, except for the 6^+ state which was taken to be the single neutron configuration $(g_{9/2}$-$i_{13/2}^{-1})$, prominent in the lowest 2^+, and dominant in the 4^+ state. The second group consists of the negative natural parity excitations: of these the first two 1^-, 3^-, and 7^- states and the first four 5^- states were studied. The third group contains the negative unnatural parity states, of which the first three 2^- and 6^-, and the first, second, and fourth 4^- levels, were considered. For both of these latter groups the state vectors of Kuo[51] were used. The same central and noncentral forces as in Sec. IV B were used for all groups.

Figure 15 shows the results for the first group, the even natural parity excitations. Except for the second 2^+ state, the strengths of the states are underestimated by an order of magnitude. This should be compared with Fig. 11, where some of the same states are examined using transition densities obtained from e-e', and the N/Z prescription for getting neutron transition den-

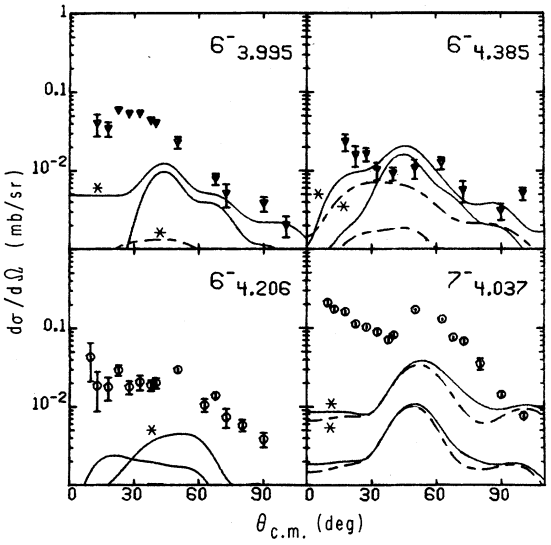

FIG. 14. The calculations using phenomenological wave functions for the states shown. The meaning of the asterisks is the same as in Fig. 10.

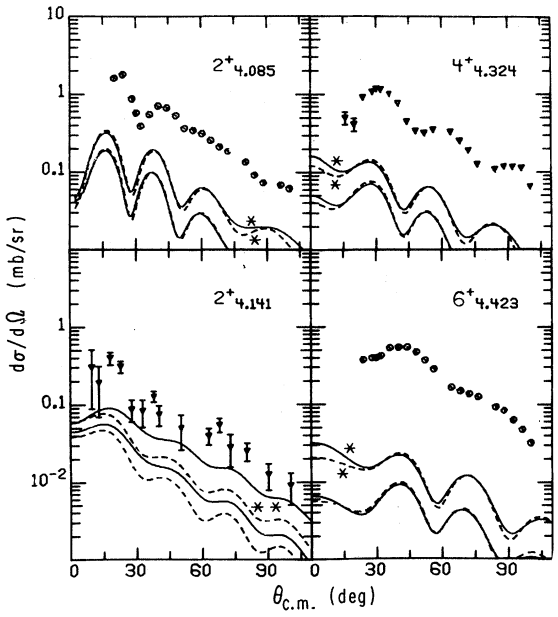

FIG. 15. Calculations for the indicated states using theoretical wave functions as cited in the text. The curves are labeled with asterisks as described in Fig. 10.

sities from proton transition densities. As pointed out in Sec. IV A, this demonstrates that for these states p-p' is in agreement with e-e'. So the microscopic wave functions are not collective enough. The introduction of many more particle-hole configurations, via the Green's function method, increases the collectivity of the 2^+ state, but is relatively ineffective for the 4^+ and 6^+ states.[52] The second 2^+ state is less strongly excited than the others and, as is seen in Fig. 15, the theoretical prediction agrees well with experiment in angular distribution, and misses only by a factor ~2 in magnitude. Noncentral forces contribute substantially to the cross section even though it is a natural parity excitation, due to the large spin-flip amplitude of the proton $(h_{9/2}$-$h_{11/2}^{-1})$ configuration, which is theoretically the largest component (amplitude 0.88) of the wave function. The moderate correlation between theory and experiment for the state suggests that this may in fact be the dominant component.

Figures 16 and 17 show the comparison of theory and experiment for the second group, the negative natural parity states. Unlike the phenomenological wave functions used in Sec. IV B, with results shown in Figs. 12–14, the random phase approximation (RPA) vectors have a large number of components, which give rise to coherent collective excitations: Over-all, agreement with theory and experiment is good, though the fractionation of strength among states of the same spin-parity is not given precisely, particularly for the 5^- states. Noteworthy is the good agreement for the lowest 5^- state which, as is pointed out in Sec. IV A and illustrated in Fig. 11, does not have a neutron transition density obeying the N/Z rule, with respect to the proton transition density, though it is a very collective state with a $B(E5)$ of 12.5 s.p.u. The RPA vector correctly describes the behavior giving good agreement for both p-p' and e-e'. Also notable is the good agreement for the very collective $(BE3 \simeq 40$ s.p.u.$)3^-$ state at 2.615 MeV, and the fact that the strength, though not the detailed angular distribution, is predicted for the 7^- states. For the 1^- states again the strengths, but not the angular distributions, are in agreement with experiment. The unusual theoretical angular distribution for the first 1^- state is due to the radial extension of the neutron spin-flip density beyond the non-spin-flip density, the cross section being dominated by the spin-flip density at forward angles.

Figure 18 displays the results for the negative unnatural parity states. The RPA state vectors for the lowest 2^-, 4^-, and 6^- states are given in Table III, compared with the phenomenological wave functions. The tensor force completely dominates the excitation of these states. The lowest

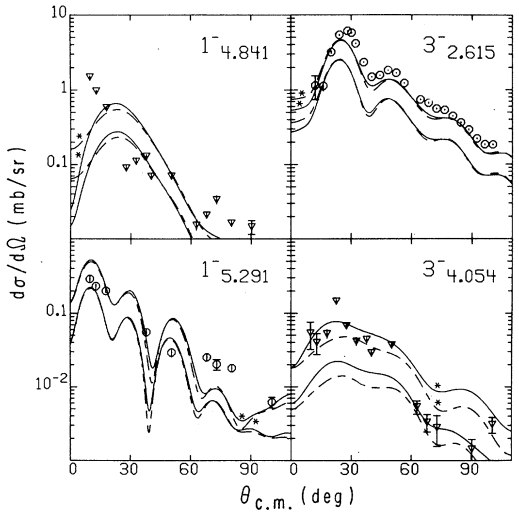

FIG. 16. Calculations for the indicated states using theoretical wave functions as cited in the text. The curves are labeled with asterisks as described in Fig. 10.

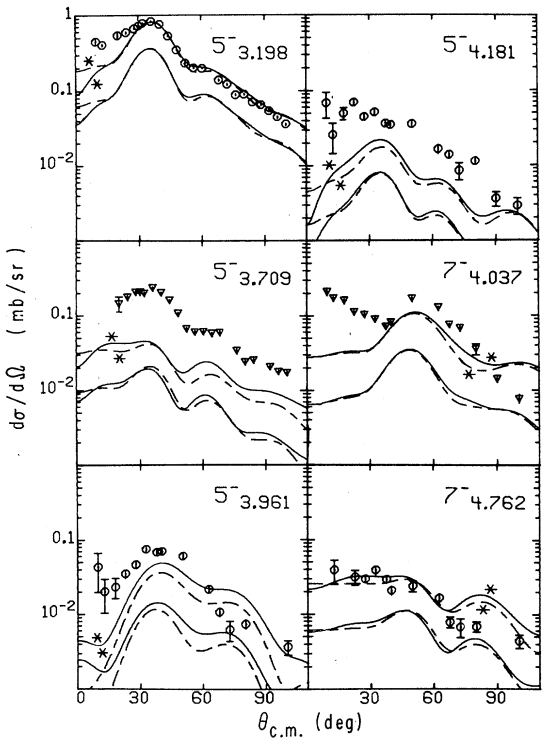

FIG. 17. Calculations for the indicated states using theoretical wave functions as cited in the text. The curves are labeled with asterisks as described in Fig. 10.

2^- and 4^- states fit fairly well but, as comparison with Fig. 12 shows, not as well as when the phenomenological wave functions are used. The excitation of these spin-flip states displays sensitivity to the main configurations involved, unlike the collective states, which depend on large numbers of configurations with small amplitudes, and which give angular distributions identical to those given by the collective model.

V. CONCLUSION

^{208}Pb was studied by high resolution proton inelastic scattering. Excitation energies and angular distributions were obtained for about 150 resolved levels. Angular momentum transfer information and deformation parameters were extracted via collective model fits to about 75 of the angular distributions. New spin-parity assignments were made for a number of levels on this basis, and many previous assignments were confirmed. In addition, comparison with experimental (e, e') results and theoretical predictions allowed identification of one magnetic dipole state and tentative identification of another.

The strongest normal parity states were studied using transition densities inferred from (e, e') experiments. Predicted angular distributions were in good agreement with the (p,p') data for excitations with angular momentum transfer ranging from two to six units, a larger range than had

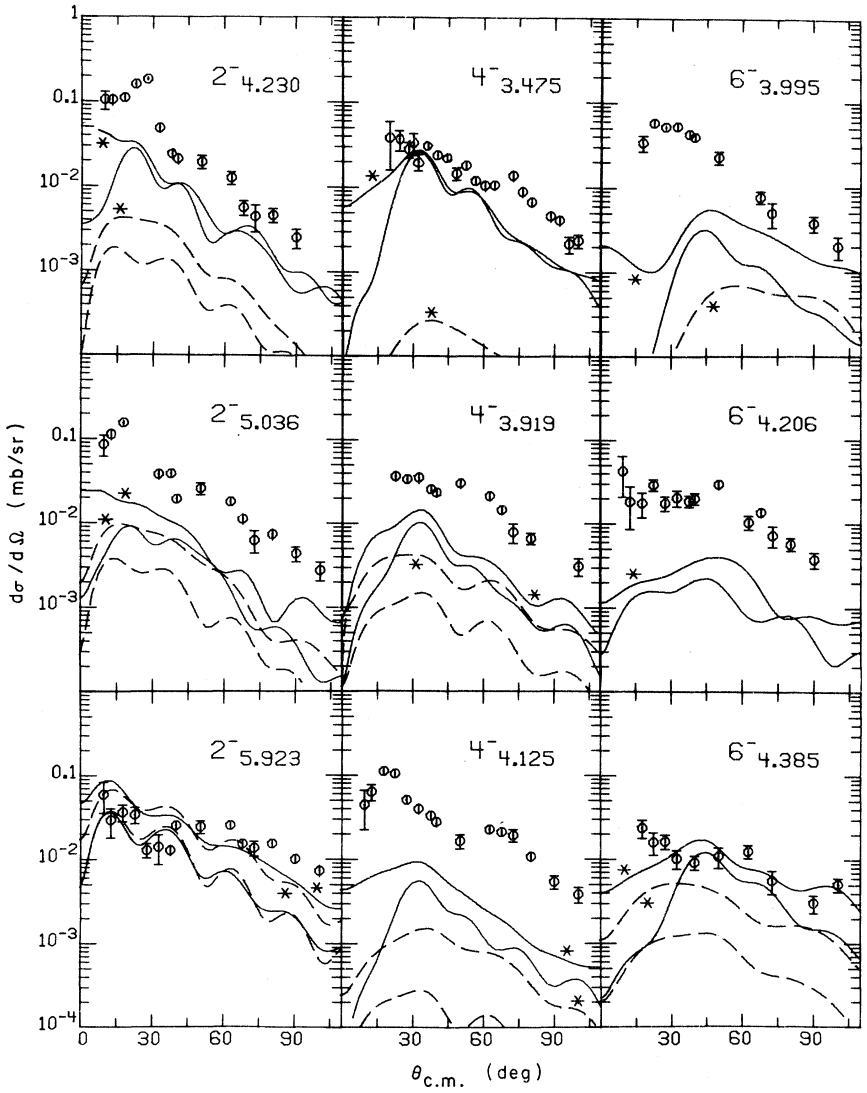

FIG. 18. Calculations for the indicated states using theoretical wave functions as cited in the text. The curves are labeled with asterisks as described in Fig. 10.

previously been examined with this technique in a single nucleus. Good results were also obtained for the strong odd normal parity states when RPA wave functions were used in the calculations. Angular distribution strengths for the strong even normal parity state were considerably underestimated by the RPA calculations, but by amounts which were consistent with those wave functions' underestimates of (e, e') form factors and electromagnetic transition rates.

The importance of noncentral parts of the projectile-target interaction was examined. The spin-orbit force used here made no significant contribution in any of the cases considered, and the tensor force had little influence on the calculations for the normal parity states, especially when the transition was strong. However, for abnormal parity excitations the tensor force had a large—often completely dominant—effect on the strength and shape of the angular distributions. The present data should provide a good testing ground for tensor forces derived from the free two-nucleon interaction.

Except for the lowest states of a given spin-parity, the cross sections of the abnormal parity states and most of the weakly excited normal parity states were underestimated by the microscopic calculations, often by large factors. Determination of whether these underestimates reflect deficiencies in the forces and wave functions used in the present calculations or result from neglect of more complicated reaction mechanisms, such as two-step processes, must await further study.

---

*Work supported in part by the National Science Foundation.

[1]J. Saudinos, G. Vallois, O. Beer, M. Gendrot, and P. Lopato, Phys. Lett. 22, 492 (1966); J. Saudinos, G. Vallois, and O. Beer, Nucl. Appl. 3, No. 2, 22 (1967); G. Vallois, Centre d'Etudes Nucleaires de Saclay, Report No. CEA-R-3500, 1968 (unpublished).

[2]M. Lewis, F. Bertrand, and C. B. Fulmer, Phys. Rev. C 7, 1966 (1973).

[3]J. Alster, Phys. Lett. 25B, 459 (1967); G. Bruge, J. C. Faivre, H. Faraggi, and A. Bussiere, Nucl. Phys. A146, 597 (1970); R. A. Moyer, B. L. Cohen, and R. C. Diehl, Phys. Rev. C 2, 1898 (1970); L. Cranberg, T. Oliphant, J. Levin, and C. Zafiratos, Phys. Rev. 159, 969 (1967), and references therein.

[4]A. Scott and M. P. Fricke, Phys. Lett. 20, 654 (1966).

[5]N. P. Mathur, Ph.D. thesis, Univ. of Delhi, 1969 (unpublished).

[6]O. Karban, P. D. Greaves, V. Hnizdo, J. Lowe, and G. W. Greenlees, Nucl. Phys. A147, 461 (1970).

[7]E. Grosse, M. Dost, K. Haberkant, J. W. Hertel, H. V. Klapdor, H. J. Korner, D. Proetel, and P. von Brentano, Nucl. Phys. A174, 525 (1971).

[8]P. Mukherjee and B. L. Cohen, Phys. Rev. 127, 1284 (1962); J. Bardwick and R. Tickle, *ibid.* 161, 1217 (1967).

[9]G. Igo, P. D. Barnes, and E. R. Flynn, Ann. Phys. (N.Y.) 66, 60 (1971); Phys. Rev. Lett. 24, 470 (1970).

[10]E. D. Earle, A. J. Ferguson, G. van Middelkoop, and G. A. Bartholomew, Phys. Lett. 32B, 471 (1970).

[11]M. Dost and W. R. Hering, Phys. Lett. 26B, 443 (1968).

[12]P. Richard, P. von Brentano, H. Weimen, W. Wharton, W. G. Weitkamp, W. W. McDonald, and D. Spalding, Phys. Rev. 183, 1007 (1969).

[13]C. F. Moore, J. G. Kulleck, P. von Brentano, and F. Rickey, Phys. Rev. 164, 1559 (1967).

[14]J. G. Cramer, P. von Brentano, G. W. Philips, H. Ejiri, S. M. Ferguson, and W. J. Braithwaite, Phys. Rev. Lett. 21, 297 (1968).

[15]G. R. Satchler, Comments Nucl. Part. Phys. 5, 39 (1972); F. Petrovich, Ph.D. thesis, Michigan State University, 1970 (unpublished); D. Agassi and R. Schaeffer, Phys. Lett. 26B, 703 (1968).

[16]H.G. Blosser, G.M. Crawley, R. de Forest, E. Kashy, and B. H. Wildenthal, Nucl. Instrum. Methods 91, 61 (1971).

[17]W. A. Lanford, W. Benenson, G. M. Crawley, E. Kashy, I. D. Proctor, and W. F. Steele, Bull. Am. Phys. Soc. 17, 895 (1972).

[18]F. D. Becchetti, Jr., and G. W. Greenlees, Phys. Rev. 182, 1190 (1969).

[19]FORTRAN programs written by G. Hamilton, Michigan State University (unpublished) and by J. A. Rice, Ph.D. thesis, Michigan State University, 1973 (unpublished).

[20]M. B. Lewis, Nucl. Data B5 (No. 3), 243 (1971).

[21]A. Heusler and P. von Brentano, Ann. Phys. (N.Y.) 75, 381 (1973); A. Heusler (private communication).

[22]G. R. Satchler, R. H. Bassel, and R. M. Drisko, Phys. Lett. 5, 256 (1963).

[23]M. P. Fricke and G. R. Satchler, Phys. Rev. 139, 567 (1965).

[24]S. A. Fulling and G. R. Satchler, Nucl. Phys. A111, 81 (1968).

[25]L. N. Blumberg, E. E. Gross, A. von der Woude, A. Zucker, and R. H. Bassel, Phys. Rev. 147, 812 (1966); R. C. Barrett, A. D. Hill, P. E. Hodgson, Nucl. Phys. 62, 133 (1965); G. W. Greenlees and G. J. Pyle, Phys. Rev. 149, 836 (1966); D. L. Watson, J. Lowe, J. C. Dore, R. M. Craig, and D. J. Baugh, Nucl. Phys. A92, 193 (1967); G. R. Satchler, *ibid.* 92, 273 (1967); G. W. Greenlees, V. Hnizdo, O. Karban, J. Lowe, and W. Makofske, Phys. Rev. C 2, 1063 (1970).

[26]F. Perey (unpublished).

[27]P. D. Kunz, University of Colorado (unpublished).

[28]C. D. Bowman, R. J. Baglan, B. L. Berman, and T. W. Philips, Phys. Rev. Lett. 25, 1302 (1970); R. E. Toohey and H. E. Jackson, Phys. Rev. C 6, 1440 (1972); A. Wolf, R. Moreh, A. Nof, O. Shahal, and J. Tenenbaum, *ibid.* 6, 2276 (1972); F. E. Cecil, Ph.D. thesis, Princeton University, 1972 (unpublished).

[29]L. W. Fagg, W. F. Bendel, E. C. Jones, N. Ensslin, and F. E. Cecil, in *Proceedings of the International Conference on Nuclear Physics*, edited by J. de Boer

and H. J. Mang (North-Holland, Amsterdam, 1973), Vol. 1, p. 631.
[30]R. A. Broglia, A. Molinari, and B. Sorenson, Nucl. Phys. A109, 353 (1968).
[31]J. D. Vergados, Phys. Lett. 36B, 12 (1971).
[32]V. Gillet, A. Green, and E. Sanderson, Nucl. Phys. 88, 321 (1966).
[33]G. R. Satchler, Comments Nucl. Part. Phys. 5, 145 (1972).
[34]A. M. Bernstein, in *Advances in Nuclear Physics*, edited by M. Baranger and E. Vogt (Plenum, New York, 1969), Vol. 3, p. 325.
[35]G. R. Hammerstein, R. H. Howell, and F. Petrovich, Nucl. Phys. A213, 45 (1973).
[36]F. Petrovich, Ph.D. thesis, Michigan State University (unpublished); F. Petrovich, H. McManus, V. A. Madsen, and J. Atkinson, Phys. Rev. Lett. 22, 895 (1969).
[37]M. Nagao and Y. Torizuka, Phys. Lett. 37B, 383 (1971).
[38]J. H. Heisenberg and I. Sick, Phys. Lett. 32B, 249 (1970).
[39]H. Rothhaas, J. Friedrich, K. Merle, and B. Dreher (unpublished).
[40]J. F. Ziegler and G. A. Peterson, Phys. Rev. 165, 1337 (1968); J. Friedrich, Nucl. Phys. A191, 118 (1972).
[41]G. R. Satchler, Phys. Lett. 35B, 279 (1971); R. H. Howell and A. I. Galonsky, Phys. Rev. C 5, 561 (1972); R. A. Hinrichs, D. Larson, B. M. Preedom, W. G. Love, and F. Petrovich, *ibid.* 7, 1981 (1973).
[42]R. Schaeffer and J. Raynal (unpublished).
[43]W. T. Wagner, G. R. Hammerstein, G. M. Crawley, J. R. Borysowicz, and F. Petrovich, Phys. Rev. C 8, 2504 (1973).
[44]G. Love, L. Parish, and A. Richter, Phys. Lett. 31B, 167 (1970).
[45]S. M. Austin, in *The Two-Body Force in Nuclei*, edited by S. M. Austin and G. M. Crawley (Plenum, New York, 1972).
[46]G. M. Crawley, S. M. Austin, W. Benenson, V. A. Madsen, F. A. Schmittroth, and M. J. Stomp, Phys. Lett. 32B, 92 (1970).
[47]S. H. Fox and S. M. Austin (to be published); S. H. Fox, Ph.D. thesis, Michigan State University (unpublished).
[48]P. Richard, W. Weitkamp, W. Wharton, H. Wieman, and P. von Brentano, Phys. Lett. 26B, 8 (1967).
[49]D. A. Bromley and J. Weneser, Comments Nucl. Part. Phys. 2, 151 (1968).
[50]W. True, C. Ma, and W. Pinkston, Phys. Rev. C 3, 2421 (1971).
[51]T. T. S. Kuo (private communication).
[52]G. F. Bertsch and S. F. Tsai, Phys. Rep. 18C, 125 (1975).